

Geophysical exploration to estimate conductivity and permittivity model of an excavated soil block

F. Uribe^a, P. Zúñiga^a, P. Gómez^b

^a*Departamento de Ingeniería Mecánica Eléctrica, Maestría en Ciencias en Ingeniería Eléctrica, CUCEI, Universidad de Guadalajara,*

Bld. Marcelino García Barragán 1421, Col. Universitaria, 44430 Guadalajara, Jal. México.

^b*Departamento de Ingeniería Eléctrica, Sección de Estudios de Posgrado e Investigación, Escuela Superior de Ingeniería Mecánica y Eléctrica Instituto Politécnico Nacional, Unidad Profesional Adolfo López Mateos, Av. I.P.N., Col. Lindavista, 07738 México, D.F. México.*

Received 25 April 2013; accepted 3 October 2013

An electrical model for a real stratified soil block is proposed in this paper. The model is suitable to estimate the physical properties of electrical conductivity and permittivity, as well as the thickness of each of the layers of the subsoil. For the estimation, we implement a methodology based on the efficient numerical solution of the Takahashi et al. infinite integrals for calculating the vector potentials at the soil surface. For the truncation of the infinite integrals, a new exponential based truncation criterion is proposed. Subsequently, to evaluate a more accurate fitting of the apparent resistivity curves obtained by measurements and by the Takahashi et al., integrals, two numerical optimization techniques based on genetic algorithms, and least squares method are implemented for accuracy assessment. Finally, a formal quantitative validation methodology is presented in this paper based on the comparison of the numerical optimization results with respect to a data set obtained by direct measurements of the electrical resistivity on the vertical excavation profiles on each subsurface layer down the experimental workstations named *Site-1, 2, ... 4*.

Keywords: Direct current ground resistance measurements; Wenner method; ground parameter estimation; genetic algorithms; least-squares optimization.

En este artículo se propone el modelo eléctrico de un bloque de suelo real estratificado basado en la estimación de sus propiedades físicas de conductividad y permitividad eléctrica así como del grosor de cada una de las capas de tierra que conforman el subsuelo. Para dicha estimación, se implementa una metodología basada en la solución numérica eficiente de las integrales infinitas de Takahashi et al. para el cálculo del potencial vectorial en la superficie del subsuelo. Para la evaluación numérica de estas integrales infinitas se propone un criterio de truncamiento basado en la función exponencial. Posteriormente, para encontrar el ajuste más preciso entre las curvas de resistividad aparente obtenidas por mediciones y por la solución numérica de dichas integrales, se utilizan por comparación dos técnicas de optimización numérica basadas tanto en algoritmos genéticos como en mínimos cuadrados. Finalmente, se presenta una validación cuantitativa formal de la metodología aquí propuesta basada en la comparación de los resultados obtenidos de la optimización numérica con respecto a los nuevos datos de resistividad eléctrica obtenidos por medición directa sobre los perfiles verticales de cada una de las capas del subsuelo en las excavaciones realizadas bajo las estaciones de trabajo experimentales denominadas como *Sitio-1, 2, ... 4*.

Descriptores: Medición de resistencia de suelo con corriente directa; método de Wenner; estimación de parámetros del suelo; algoritmos genéticos; optimización por mínimos cuadrados.

PACS: 93.85.Fg; 91.60.-x; 77.22.Ch; 84.37.+q

1. Introduction

An accurate characterization of the physical properties of sub-surface ground layers is of great importance in geophysics prospecting for many different applications such as ground penetrating radar (GPR) [1], electromagnetic propagation in the presence of a stratified soil [2], seismic wave propagation in stratified media [3], ground grids design for electrical protection [4], among others.

The representation of a conductor or dielectric material in the ground sub-surface media is better described by the frequency dependent complex relative permittivity ($\epsilon_r^*(\omega)$). Several frequency dependent effects on mode wave propagation such as attenuation, polarization, dispersion, relaxation and resonance are well represented with this physical model [5]. Meanwhile, the real component of this model represents

energy dissipation, and the imaginary one represents energy storage.

The former is related to the electrical conductivity of the material or media (σ), and the latter is directly related to the relative permittivity factor, better known as the material dielectric constant or permittivity constant (ϵ_r) [5].

Thus, several methods are used to measure the electromagnetic properties of the earth from its surface; these range from direct current ground resistivity techniques to radio frequency exploration [6-7].

For the interpretation and estimation of a certain apparent resistivity curve of a given ground block, there exist many theoretical and numerical techniques based on optimization methods to help find a more accurate fitted numerical solution [8-10].

However, none of the above cited works includes a quantitative validation to estimate the electrical parameters and width of each of the subsoil subsurface layers through excavations of a ground block *in situ*.

Thus, an accurate methodology to estimate the electrical parameters as well as the ground layer widths of a real stratified ground block is presented in this paper. For such an estimation, the Takahashi *et al.* [8] integrals are numerically solved using a new efficient exponential truncation criterion.

Then, the obtained apparent resistivity curve is optimized by means of Genetic algorithms (GA) [9] and least-squares technique (LS) [10], which yields an error below 9% for the sampled range.

In addition, measurements are taken each 20 cm of electrode distance at the soil surface via the Wenner method. After an identification of the samples composition of each ground layer material (extracted from the excavations), a correspondence with a reference data table taken from [1] and [11] is used to estimate the magnitude of each ground layer dielectric constant (ϵ_r).

Finally, the results obtained in this work are validated through excavations performed under a real ground block to obtain the width, ground resistivity and water content of each ground layer.

2. Measurement and interpretation of the apparent resistance curve via the Wenner method

To evaluate the physical properties of a ground surface location, we first proceed to trace a path to delimit the area of interest for the analysis. Then, a set of parallel and horizontal surface measurements of ground resistivity curves are taken along the four experimental stations named *Site-1* through *Site-4*, using a direct current electronic tester [4].

The ground resistivity measurements were performed within the facilities of the State University of Guadalajara, CUCEI campus, placed in Guadalajara, Jalisco, Mexico with coordinates $20^\circ 41'$ north latitude and $103^\circ 20'$ west longitude, as shown in Fig. 1a.

Thereafter, using civil engineering equipment we proceeded to perform excavations beneath each of the experimental workstations as is shown in Fig. 1b, in order to corroborate the ground apparent resistivity profiles obtained initially from ground surface horizontal measurements, over each workstation as shown in Fig 2a.

In addition, measurements on each of the ground layer vertical profiles down experimental workstations *Site-1-4* were taken as illustrated in Fig. 2b. The measurements inside the excavations are further used in Sec. 7 as a physical evidence for a quantitative validation of the ground resistivity data measured in a horizontal path initially from the ground surface over each workstation.

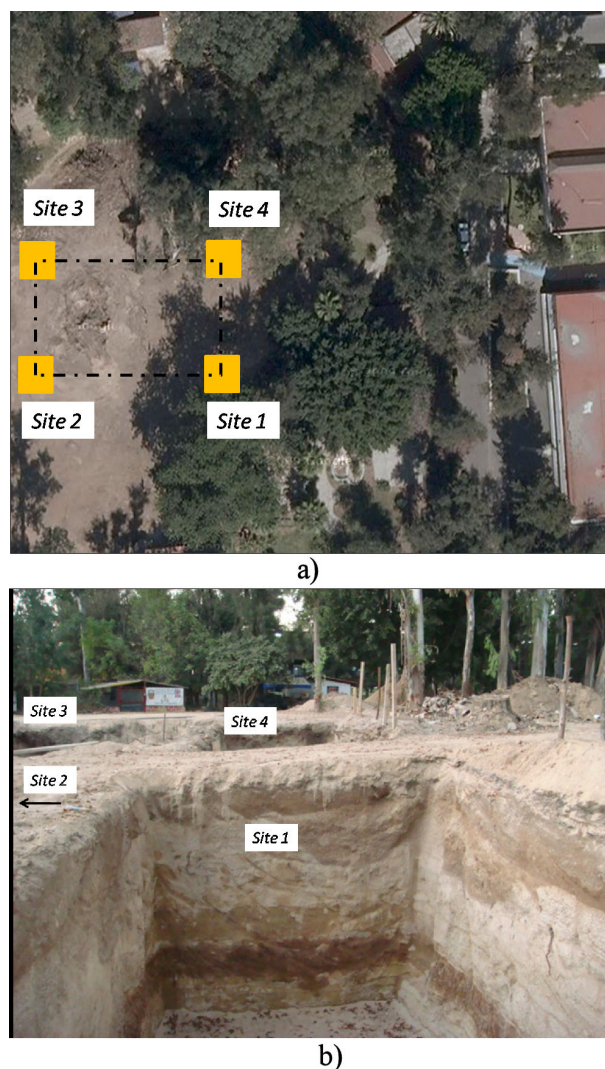


FIGURE 1. Geographic location. a) Four monitoring experimental stations named *Site-1-4*. b) Excavations below each experimental station.

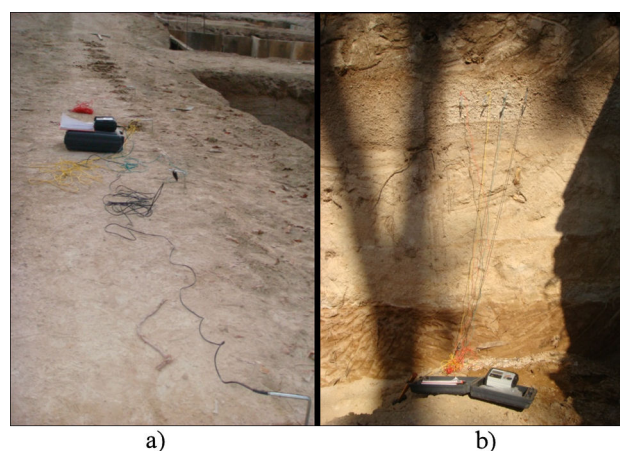


FIGURE 2. Apparent resistivity curve measurements. a) Horizontal measurements taken from the soil surface. b) Vertical measurements on each of the stratified profiles down experimental workstation *Site-1*.

TABLE I. Four layer parameter set (Site-1)

| n | Empirical Interpretation | | Numerical Optimization (Genetic Algorithm) | | Validation Measurements | |
|-----|-------------------------------------|-----------------|--|----------------------|---------------------------------------|-------------------|
| | ρ_{h-Mes} ($\Omega \cdot m$) | h_{n-Mes} (m) | $\rho_{c-Optim-GA}$ ($\Omega \cdot m$) | $h_{n-Optim-GA}$ (m) | $\rho_{m-Valid}$ ($\Omega \cdot m$) | $h_{n-Valid}$ (m) |
| 1 | 105 | 0.60 | 103.60 | 0.8812 | 134 | 0.60 |
| 2 | 600 | 1.20 | 767.66 | 0.9020 | 682 | 0.65 |
| 3 | 300 | 1.80 | 177.22 | 1.6322 | 147 | 1.52 |
| 4 | 50 | ∞ | 11.603 | ∞ | 16.8 | ∞ |

TABLE II. Three layer parameter set (Site-2)

| n | Empirical Interpretation | | Numerical Optimization (Genetic Algorithm) | | Validation Measurements | |
|-----|-------------------------------------|-----------------|--|----------------------|---------------------------------------|-------------------|
| | ρ_{h-Mes} ($\Omega \cdot m$) | h_{n-Mes} (m) | $\rho_{c-Optim-GA}$ ($\Omega \cdot m$) | $h_{n-Optim-GA}$ (m) | $\rho_{m-Valid}$ ($\Omega \cdot m$) | $h_{n-Valid}$ (m) |
| 1 | 103 | 0.50 | 102.45 | 0.4810 | 106.2 | 0.60 |
| 2 | 357 | 1.20 | 354.42 | 1.0237 | 382.4 | 1.45 |
| 3 | 78 | ∞ | 74.606 | ∞ | 92.4 | ∞ |

TABLE III. Four layer parameter set (Site-3)

| n | Empirical Interpretation | | Numerical Optimization (Genetic Algorithm) | | Validation Measurements | |
|-----|-------------------------------------|-----------------|--|----------------------|---------------------------------------|-------------------|
| | ρ_{h-Mes} ($\Omega \cdot m$) | h_{n-Mes} (m) | $\rho_{c-Optim-GA}$ ($\Omega \cdot m$) | $h_{n-Optim-GA}$ (m) | $\rho_{m-Valid}$ ($\Omega \cdot m$) | $h_{n-Valid}$ (m) |
| 1 | 90 | 0.80 | 101.70 | 1.6034 | 101.4 | 0.72 |
| 2 | 140 | 1.60 | 201.46 | 1.3464 | 162.8 | 1.45 |
| 3 | 100 | 2.80 | 202.71 | 1.6109 | 117.2 | 2.52 |
| 4 | 45 | ∞ | 37.920 | ∞ | 39.8 | ∞ |

TABLE IV. Three layer parameter set (Site-4)

| n | Empirical Interpretation | | Numerical Optimization (Genetic Algorithm) | | Validation Measurements | |
|-----|-------------------------------------|-----------------|--|----------------------|---------------------------------------|-------------------|
| | ρ_{h-Mes} ($\Omega \cdot m$) | h_{n-Mes} (m) | $\rho_{c-Optim-GA}$ ($\Omega \cdot m$) | $h_{n-Optim-GA}$ (m) | $\rho_{m-Valid}$ ($\Omega \cdot m$) | $h_{n-Valid}$ (m) |
| 1 | 90 | 1.60 | 97.837 | 2.2665 | 98.2 | 1.46 |
| 2 | 120 | 1.90 | 132.77 | 1.7048 | 132.4 | 1.5 |
| 3 | 90 | ∞ | 105.98 | ∞ | 117 | ∞ |

Thus, the first objective of this paper methodology is to perform a detailed sampling of the different ground surface layers down the excavated workstations Site-1, 2, ... 4.

Further, ground resistance measurements ($R = V/I$) were taken along 5 m using uniform increments of 0.2 m with the Wenner method as illustrated in Fig. 3a [3].

Subsequently, the apparent resistivity curve $\rho_{h-Mes} = 2\pi h \cdot R$ is calculated from actual measurement data, as shown in

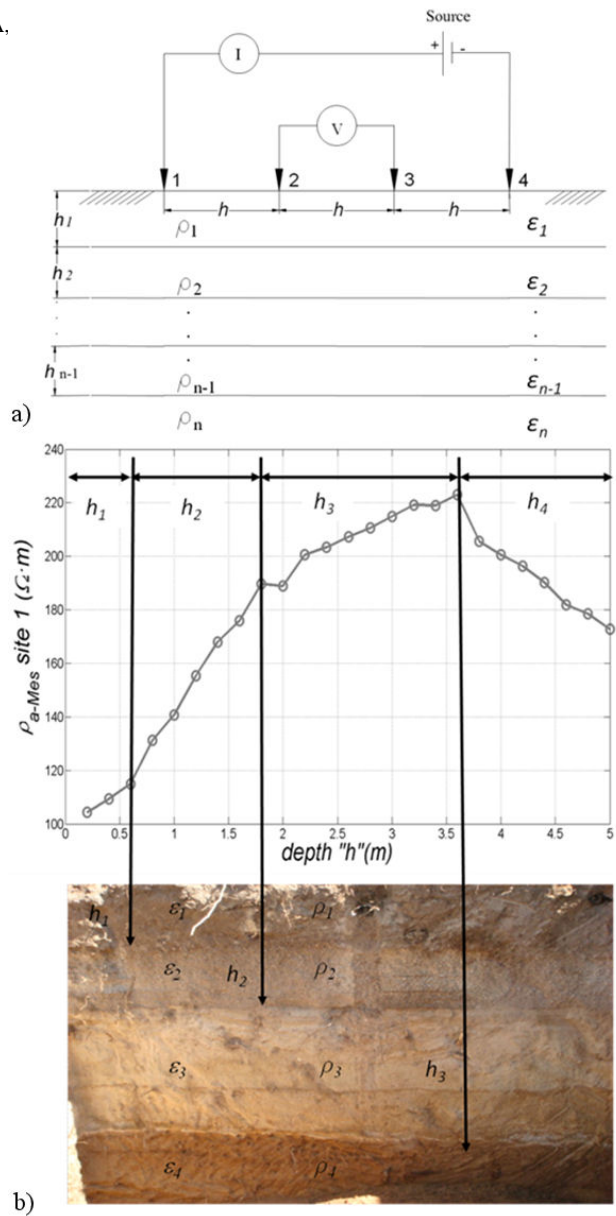


FIGURE 3. Electrical parameter measurements and empirical interpretation of the apparent resistivity curve. a) Bases of Wenner method. b) Magnitude of measurements for each ground layer below experimental workstation Site-1.

Fig. 3b (h is the horizontal distance between electrodes which also corresponds to the ground depth test).

From the slope changes of curve ρ_{h-Mes} in the top of Fig. 3b an initial empirical guess for the interpretation of the ground layer width and apparent resistivity is performed for Site-1, 2, ... 4. The results of this empirical interpretation are listed in the first (left hand side) column of Tables I to IV. The second and third columns of each table are the corresponding layer parameter magnitudes for each experimental workstation from Site-1 to 4 calculated through numerical optimization and validation measurements, further explained in the following paper sections.

3. Parameter estimation by numerical integration

As it usually occurs in engineering practice, the magnitude correspondence between the empirically interpreted parameter curve and the measured one ρ_{h-Mes} remains uncertain. Thus, we have to calculate a new estimated resistivity curve based on a formal mathematical theoretical solution.

Takahashi *et al.* proposed that the ground surface potential at any point V_0 (in cylindrical coordinates), assuming a homogeneous and isotropic soil resistivity ρ_0 due to a circulating current I , is well described by [8]:

$$V_0 = \frac{\rho_0 I}{2\pi} \int_0^\infty e^{-|z|\lambda} J_0(x\lambda) d\lambda \quad (1a)$$

where λ is the integrating variable, x is the distance between electrodes and J_0 is the zero order first class Bessel function [8]. The potential at any point of the ground surface is given by:

$$V_N(x) = \frac{\rho_1 I}{2\pi x} [1 + F_N(x)] \quad (1b)$$

where

$$F_n(x) = 2x \int_0^\infty \frac{k_{n1} e^{-2h_1 \lambda}}{1 - k_{n1} e^{-2h_1 \lambda}} \cdot J_0(\lambda x) d\lambda \quad (1c)$$

and the apparent resistivity [8]:

$$\rho_{c-Est} = \rho_1 [1 + 2F_n(h) - F_n(2h)] \quad (1d)$$

Function $F_n(x)|_{x=h,2h,3h,\dots}$ is the Takahashi *et al.* ground surface potential integral calculated for every point of the ground surface and K_{n1} are the multiple layer reflection coefficients described in [8].

Since the upper limit of the integral in (1a) is infinite, the numerical solution requires a truncation limit. This quantity affects both the solution error and the computational time. Thus, an efficient truncating criterion to solve the upper infinite limit in (1a) is proposed in this section. The use of this proposed criterion yields a fast and accurate numerical integration solution that can be solved through any quadrature routine, *e.g.* the trapezoidal rule.

After some algebraic manipulations, (1a) can be expressed as a factor of a damping and an oscillatory term, where the former determines the magnitude of the integral for the infinite range as follows:

$$\int_0^\infty e^{-\alpha\lambda} d\lambda = \int_0^{\lambda_{max}} e^{-\alpha\lambda} d\lambda + \int_{\lambda_{max}}^\infty e^{-\alpha\lambda} d\lambda \quad (2a)$$

where $\alpha = 2\Delta h_1$ and the new integration truncated range is given by:

$$\begin{aligned} \int_0^{\lambda_{max}} e^{-\alpha\lambda} d\lambda &= \int_0^\infty e^{-\alpha\lambda} d\lambda - \int_{\lambda_{max}}^\infty e^{-\alpha\lambda} d\lambda \\ &= -\frac{1}{\alpha} (e^{-\alpha\lambda_{max}} - 1) \end{aligned} \quad (2b)$$

Thus, the error term for the new truncated range is:

$$\text{Error} = \frac{1}{\alpha} e^{-\alpha\lambda_{max}} \quad (2c)$$

In consequence, the following exponential criterion is used:

$$\lambda_{max} = -\frac{\ln(2h_1 \cdot \text{Error})}{2h_1} \quad (2d)$$

where h_1 is the width of the first ground layer thickness. A reasonable Error = 1×10^{-6} is considered low enough for this application.

4. Genetic Algorithm and Least Squares Numerical Optimization

There are two main types of error sources when measuring the apparent soil resistivity with an electrical direct current equipment [6]. On one hand, it is possible that the electrodes are not tightly driven into the soil due to a rocky ground type. On the other hand, the path measurements are not accurately traced with the electrodes due to the roughness of the terrain or in the presence of near natural water ponds.

Figure 4 shows the calculated soil apparent resistivity curves ρ_{c-Est} and the measured apparent resistivity curves ρ_{h-Mes} for the four experimental workstations *Site* – 1, 2, . . . 4 .

As it can be seen in this figure, these curves do not match each other. This problem is overcome in this paper through numerical optimization, in order to adjust the new calculated curves $\rho_{c-Optim}$ with the previously measured curves ρ_{h-Mes} [9,10].

To assess the accuracy between both curve set, the following relative error criterion is used [5]:

$$\% \varepsilon_{rel} = \sum_{k=1}^n \left| 1 - \frac{\rho_{c-Est,Optim_k}}{\rho_{h-Mes_k}} \right| \times 100 \quad (3)$$

For simplicity, in the case of optimizing a new curve set $\rho_{c-Optim-LS}$ with $2N - 1$ variables we also choose to apply the least-squares method (LS) implemented from available routines in Matlab [12]. The numerical accuracy of the estimation is evaluated here through the relative error criterion ($\% \varepsilon_{rel}$) in (3) for the ρ_{h-Mes} . Obtained results are shown in Fig. 5.

In addition, we also implemented the Genetic Algorithms Matlab routines (GA) [12], to calculate the new parameter curve sets $\rho_{c-Optim-GA}$ which are also shown in Fig. 5 and listed in the second column of Table I, II, . . . , IV.

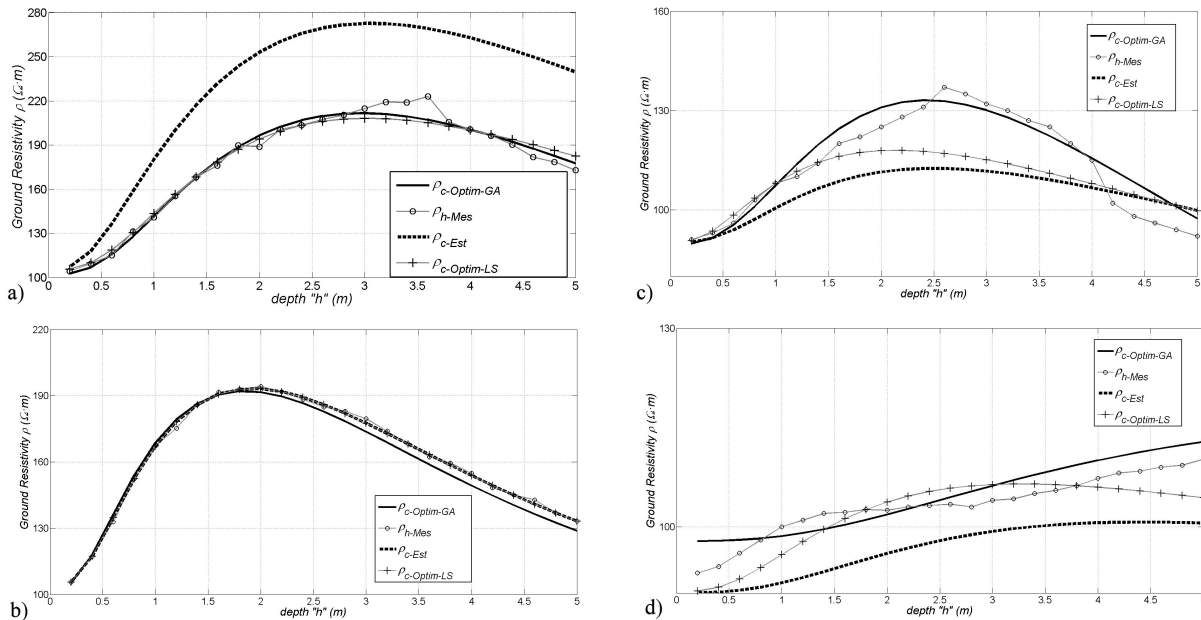


FIGURE 4. Ground resistivity curve set obtained with direct measurements, numerical integration and optimization using GA and LS methods. a) Site 1. b) Site 2. c) Site 3. d) Site 4.

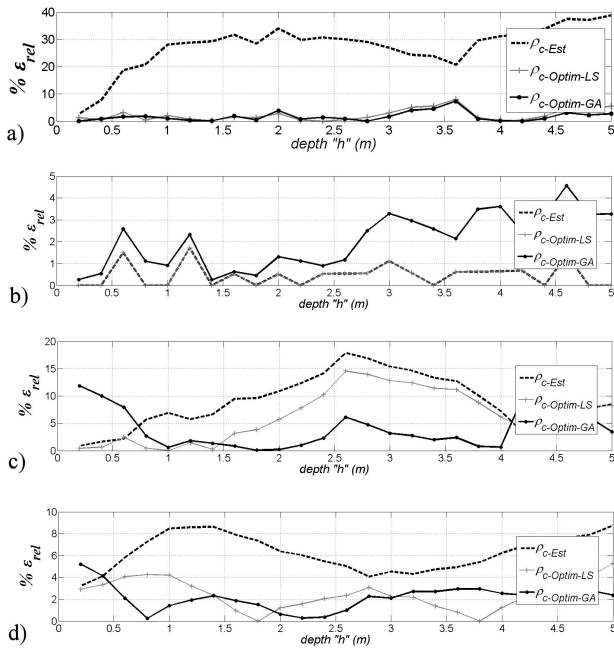


FIGURE 5. Relative error criterion ($\% \varepsilon_{rel}$) between ground resistivity curves ρ_{c-Est} , $\rho_{c-Optim-LS}$ and $\rho_{c-Optim-GA}$ with respect to the measurement master curve ρ_{h-Mes} . a) Site 1. b) Site 2. c) Site 3. d) Site 4.

5. Quantitative validation through excavations down experimental workstations Site-1, 2, ..., 4

The accuracy of the fitted resistivity curve set is validated through direct measurements performed over the vertical pro-

files on each of the different ground layers down the excavations performed beneath the experimental workstations named Site-1 to Site-4. Thus, a resistivity value is measured for each of the stratified ground layers, placing the electrodes as shown in Fig. 2b for the case of the bottom ground layer in Site-1.

On applying the Wenner method, it is assumed that the current flowing between electrodes circulates mostly through a single ground layer (following a homogeneous ground resistivity path), in the case when the measurement terminals are placed close enough to each other.

Thus, the resistivity values for quantitative validation ($\rho_{m-Valid}$) are shown in the right hand side of Table I, II, III and IV, corresponding to the depth of each ground layer (h). As can be seen in Table I-IV, the optimized and actual data show close agreement, which confirms the accuracy of the calculated magnitude ground resistivity values shown in Table I-IV.

6. Estimated ground layer dielectric permittivity

The high frequency ground wave propagation velocity, attenuation and delay are important quantities in geo-electrical surveying [1-2]. These wave magnitudes basically depend on the conductivity and dielectric properties of each ground layer [1]. In ground propagation surveying the frequency dependent complex relative permittivity (ε_r^*) is a measure of the capacity of a material to store and transmit energy from an incident electromagnetic (EM) field into the ground media [5]. It also represents a measure of the wave propagation into the ground depth [1,11].

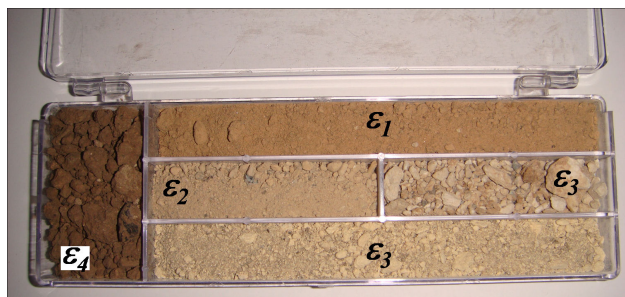


FIGURE 6. Sample holder of each of the four ground layers taken down experimental workstation *Site-1*

TABLE V. Ground dielectric constant magnitudes taken from [1,11]

| Ground Layer | Type of Samples | Literature Ranges for ϵ_r [1,11] | Estimated ϵ_r (depends of water content) |
|--------------|------------------------------------|---|---|
| 1 | Average organic-reach surface soil | 12 | 12 |
| 2 | Clay | 5-40 | 7 |
| 3 | Dry sand | 3-5 | 4 |
| 4 | Granite | 4-6 | 5 |

It is well known that the complex relative permittivity (ϵ_r^*) can be empirically estimated, measured in laboratory using a spectrum analyzer, or synthesized in the frequency domain with the following relation [1,11]:

$$\epsilon_r^*(\omega) = \epsilon_r + \frac{\sigma}{j\omega\epsilon_0} \tag{1}$$

where ϵ_r is the material dielectric constant, σ is the DC electrical conductivity (S/m), ω is the angular frequency $2\pi f$ (rad/s) and ϵ_0 is the electric permittivity of the vacuum (8.854×10^{-12} F/m).

To analyze an incident electromagnetic wave on a stratified soil as the one physically evidenced in Fig. 3b, first, we have to estimate the ϵ_r value for each of the four ground resistivity layers.

Ground samples taken from each of the four ground layers down *Site-1* in Fig. 3b are shown in the sample holder in Fig. 6. As it can be seen, different natural composition for each ground layer can be found, consisting of the materials listed in the second column of Table V. In Fig. 6, ϵ_n corresponds to the constant relative permittivity of the $n - th$ layer.

The third column in Table V, shows the corresponding range values for ϵ_r of each ground sample taken from the specialized literature [1,11].

It is well known that one of the most important factors to define the magnitude ranges of the dielectric constant ϵ_r of a specific ground material is the water content [11].

The fourth column of Table V shows an empirical estimation of the ϵ_r magnitudes based on a direct observation of the low water content found in the acquired samples during excavations.

7. Conclusions

A methodology to estimate the ground layer width, electrical permittivity and conductivity for a real stratified ground block is implemented in this paper. From this methodology a numerical model applicable to many compositions of ground subsurface materials can be extended to study or to validate the accuracy of other numerical methodologies of high frequency measurements such as GPR [1]. Also, the wave propagation effects in ground such as attenuation and phase delay on stratified soil models can be validated with the methodology proposed in this paper. For the estimation of the ground layer thickness and electrical resistivity we used a DC electronic equipment to take measurements from the surface of each of the four experimental workstations. After an intuitive interpretation of the measured apparent resistivity curve we proposed a ground layer subsurface model down experimental workstations from *Site-1* to *Site-4*.

The Takahashi *et al.* infinite integrals for calculating the ground surface vector potentials were numerically solved with high accuracy, using an exponential truncation criterion.

Furthermore, to obtain a better fitting of the apparent resistivity curve we applied two numerical optimization methods: genetic algorithms (GA) and least-squares (LS). From this application case, the error computed with GA was below 9% for the entire range. However, LS method presented a better numerical performance with less than 1 s of elapsed computing time on a PC with 3 GHz and 8 Gb RAM running Matlab 7.12R [12].

For a qualitative validation of the previously estimated ground parameters we performed excavations below the four experimental workstations *Site-1-4*.

Furthermore, the measurements were performed on the vertical profile of each ground layer beneath the excavations.

From the samples taken from each ground layer on the vertical profile excavations under *Site-1-4*, we found that the natural composition of the surface depth consists basically on the following type of materials: average organic-reach surface soil, clay, dry-sand and granite. After using lookup tables from specialized literature we can relate the information between the constant relative permittivity with each of the four extracted ground layer samples.

Based on the low ground water content of the samples it has been possible to estimate a certain relative permittivity constant to synthesize the left hand side of Eq. (4).

Finally, with the estimated parameters σ , ϵ_r and h we can define a more accurate ground wave propagation model as an aid to study the high frequency ground effects during transient or steady state conditions useful for low and high frequency engineering application studies.

-
1. J.L. Davis and A.P. Annan, *Geophysical Prospecting*, **37** (1989) 531.
 2. J. R. Wait, *Electromagnetic waves in stratified media* (The Institute of Electrical and Electronic Engineers, New York, 1996).
 3. B.L.N. Kennett, *Seismic wave propagation in stratified media* (Cambridge Univ. Press, Cambridge, 1985).
 4. *IEEE Guide for Measuring Earth Resistivity, Ground Impedance and Earth Surface Potentials of a Ground System, IEEE Standard 81-1983* (The Institute of Electrical and Electronic Engineers, New York, 1983).
 5. C.A. Balanis, *Advanced engineering electromagnetics* (Wiley, New York, 1989).
 6. *IEEE Guide for Measurements of Electromagnetic Properties of Earth Media, IEEE Standard 356-2010* (The Institute of Electrical and Electronic Engineers, New York, 2011).
 7. M.N. Nabighian, *Electromagnetic Methods in Applied Geophysics*, vol. 2 (Society of Exploration Geophysicists, Tulsa, 1991).
 8. T. Takahashi and T. Kawase, *IEEE Trans. Power Delivery*, **5** (1990) 604.
 9. I.F. Gonos and I.A. Stathopoulos, *IEEE Trans. Power Delivery*, **20** (2005) 100.
 10. R.L. Lines and S. Treitel, *Geophysical Prospecting*, **32** (1983) 159.
 11. D.K. Butler, J.E. Simms, D.S. Cook, *Geo-archeology*, **9** (1994) 437.
 12. MATLAB, version 7.12 (Math Works, Inc., Natick, Massachusetts, 2003).